



1 **A study on the performance of low-cost sensors for source**
2 **apportionment at an urban background site**

3
4 **Dimitrios Bousiotis¹, David C.S. Beddows¹, Ajit Singh¹, Molly Haugen²,**
5 **Sebastián Díez³, Pete M. Edwards³, Adam Boies², Roy M. Harrison¹, and**
6 **Francis D. Pope^{1*}**
7

8 ¹Division of Environmental Health and Risk Management, School of Geography, Earth and
9 Environmental Sciences University of Birmingham, Edgbaston, Birmingham B15 2TT,
10 United Kingdom

11
12 ²Department of Engineering, University of Cambridge, Trumpington Street, Cambridge,
13 CB2 1PZ, United Kingdom

14
15 ³Wolfson Atmospheric Chemistry Laboratories, Department of Chemistry, University of
16 York, Heslington, York YO10 5DD, United Kingdom

17
18 ***Corresponding Author, correspondence to Francis Pope f.pope@bham.ac.uk**



19 **Abstract**

20 While the measurements of atmospheric pollutants are useful in understanding the level of
21 the air quality at a given area, receptor models are equally important in assessing the
22 sources of these pollutants and the extent of their effect, helping in policy making to deal
23 with air pollution problems. Such analyses were limited and were attempted until recently
24 only with the use of expensive regulatory-grade instruments. In the present study we
25 applied a two-step Positive Matrix Factorisation (PMF) receptor analysis at a background
26 site using data acquired by low-cost sensors (LCS). Using PMF, the identification of the
27 sources that affect the air quality at the background site in Birmingham provided results
28 that were consistent with a previous study at the site, even though in different measuring
29 periods, but also clearly separated the anticipated sources of particulate matter (PM) and
30 pollution. Additionally, the method supplied a metric for the contribution of different
31 sources to the overall air quality at the site, thus providing pollution source apportionment.
32 The use of data from regulatory-grade (RG) instruments further confirmed the reliability of
33 the results, as well as further clarifying the particulate matter composition and origin.
34 Comparing the results from a previous analysis, in which a k-means clustering algorithm was
35 used, a good consistency between the results was found, and the potential and limitations
36 of each method when used with low-cost sensor data are highlighted. The analysis
37 presented in this study paves the way for more extensive use of LCS for atmospheric
38 applications and receptor modelling. Here, we present the infrastructure for understanding
39 the factors that affect the air quality at a significantly lower cost than previously possible,
40 thus opening up multiple new opportunities for regulatory and indicative monitoring for
41 both scientific and industrial applications.



42 **1. Introduction**

43 Air pollution is a major problem not only affecting human health (Pascal et al., 2013; Rivas
44 et al., 2021; Shiraiwa et al., 2017; Wu et al., 2016; Zeger et al., 2008), but also causing
45 environmental deterioration and social disparity due to its effect on climate change
46 (Manisalidis et al., 2020; Mannucci and Franchini, 2017; Moore, 2009). This effect is more
47 prominent especially within the urban environment or near pollution hot spots, though
48 areas even hundreds of kilometres away from the emission sources can also be affected
49 (Valavanidis et al., 2008, Bousiotis et al., 2021). As a result, the knowledge of the sources of
50 air pollution is vital in both understanding the air quality at a given site as well as for policy
51 making and action to improve air quality. Such knowledge was provided, until now, by the
52 analysis of data from expensive regulatory grade (RG) instruments, the use of which was not
53 extensive due to their high cost and bulky size almost exclusively for scientific research. As a
54 result, there is limited knowledge of the sources that affect the air quality. This is in part due
55 to the exiguous deployment and spatial resolution of these expensive instruments
56 (Kanaroglou et al., 2005), especially in low- and middle-income countries. In these areas the
57 problem of air quality and its effect on human health is of great importance and expected to
58 further increase in the coming years as a result of their rapid industrial and population
59 growth (Kan et al., 2009; Petkova et al., 2013). To combat this, in the past decade, the
60 development of low cost sensors (LCS) measuring either PM or gas phase pollutant
61 concentrations has intensified (Lewis et al., 2018; Penza, 2019; Popoola et al., 2018), though
62 still being far from an equal alternative to the more expensive RG instruments. Many
63 limitations are associated with their use, with the main shortcoming being the inconsistency
64 of their measurements, even for similar sensors deployed at the same site (Austin et al.,
65 2015; Sousan et al., 2016), either due to operational and detector sacrifices that allow them
66 to be inexpensive or from the effect of meteorological conditions that bias their
67 measurements (Crilley et al., 2020; Hagan and Kroll, 2020; Wang et al., 2021). Thus,
68 consistent calibration (Kosmopoulos et al., 2020; De Vito et al., 2020) and data corrections
69 (Crilley et al., 2018; Liang et al., 2021; Vajs et al., 2021) are required for these sensors to
70 provide reliable measurements (though sometimes even this is not enough) in addition to
71 their continuous improvement and evolution (Giordano et al., 2021). Nevertheless, these



72 sensors have the potential to change the state of air pollution monitoring by allowing wider
73 use and better spatio-temporal coverage.

74 Many applications of LCS have been found in over the recent years providing measurements
75 at sites that were previously inaccessible by regulatory instrumentation, either due to being
76 economically difficult (Miskell et al., 2018; Omokungbe et al., 2020; Pope et al., 2018) or due
77 to the limitations set by their size (Jovašević-Stojanović et al., 2015; Nagendra et al., 2019,
78 Whitty et al., 2022). Additionally, the use of LCS made possible higher spatial resolution than
79 RG instruments (Feinberg et al., 2019; Krause et al., 2019; Prakash et al., 2021), greatly
80 improving the ability to measure air quality at more points of interest even at
81 neighbourhood scale (Schneider et al., 2017; Shafran-Nathan et al., 2019; Shindler, 2021),
82 supplementing the existing regulatory network (Weissert et al., 2020). While the
83 applications of LCS provided the information of the level of air quality at more sites, the vital
84 information of air pollution sources and the environmental conditions that enable or disable
85 air pollution, as well as their relative contributions is yet to be uncovered by their use. Pope
86 et al., (2018) using PM ratios managed to separate and identify the effect of major sources
87 of pollution in several cities in East Africa using data from LCS. Popoola et al, (2018)
88 identified the sources of pollution near Heathrow Airport, London using a network of LCS.
89 Bousiotis et al., (2021) using k-means clustering on PM data from both a LCS and an RG
90 instrument, showed the strengths and limitations of the sensor, in measuring particle
91 number concentrations and using them to identify the sources of pollution at a background
92 site in Birmingham, UK. While these studies identified many sources and conditions that
93 affected the air quality at the sites, there was no information on their temporal and relative
94 contribution.

95 In the present study, the two-step PMF (Beddows and Harrison, 2019), an advanced version
96 of a statistical method for source apportionment successfully applied in many studies with
97 RG instruments (Beddows et al., 2015; Harrison et al., 2011; Hopke, 2016; Leoni et al., 2018;
98 Pokorná et al., 2016), is applied on data collected from various LCS. This provides a
99 quantitative separation of the different sources and their contributions to a background site
100 located in Birmingham. Furthermore, data from RG instruments and an Aerosol Chemical
101 Speciation Monitor (ACSM) were also used in the analysis. This was done not only to
102 compare the results from the two sets, but to further characterise the sources of larger
103 particles at the site as well. The results of the present analysis are also compared with those



104 from a previous study at the same site made by Bousiotis et al., (2021), displaying the
105 additional information provided by the PMF as well as to check the consistency of the
106 results between the two methods. To the authors' knowledge source apportionment with
107 LCS data has only been attempted previously by Hagan et al., (2019) using Non-negative
108 Matrix Factorisation on a dataset from New Delhi, India, providing information of
109 combustion and non-combustion sources as well as their partial contributions in a three-
110 factor solution. The present work sets the ground for future use of such sensors in a variety
111 of scientific and industrial scenarios, which can make feasible their wider use either as
112 standalone sources of the data needed for such studies or in combination with RG
113 instruments for better spatial coverage.

114

115 **2. Methods**

116 **2.1 Location of the site and instruments**

117 The measurement site is the Birmingham Air Quality Supersite (BAQS) located at the
118 grounds of the University of Birmingham (52.45°N; 1.93°W) (fig. 1). This is an urban
119 background site within a large residential area about 3 km southwest of the city centre of
120 Birmingham. For this site, PM concentration measurements in the range 0.35 to 40 μm were
121 collected using an Alphasense OPC-N3 in a 10 second resolution (averaged in 1-hour
122 resolution) for the period between 16/10/2020 to 30/10/2020. Additionally, data from
123 several LCS were also collected. NO_x and ozone measurements were collected using the Box
124 Of Clustered Sensors (BOCS, Smith et al., 2019) in the same time resolution, as well as black
125 carbon (BC) concentrations using the MA200 sensor by Magee Scientific. Finally, the data for
126 the lung deposited surface area (LDSA) of particles in the range of 10 nm to 10 μm , which is
127 found to strongly correlate with BC emissions (Lepistö et al., 2022), was collected using a set
128 of two Naneos Partectors by Naneos Particle Solutions GmbH. One sensor measured the
129 surface of all particles in this size range, while the second is placed after a catalytic stripper
130 (Catalytic Instruments CS015) which removes the semi-volatile particles (Haugen et al.
131 2022).

132 Apart from the data provided directly from the sensor before the catalytic stripper, the ratio
133 between the measurements of the two Naneos Partectors was also considered according to:

134



$$LDSA_{ratio} = \frac{LDSA \text{ after the catalytic stripper}}{LDSA \text{ before the catalytic stripper}}$$

136

137 This was done to resolve whether such a configuration can provide additional information
138 for the origin of pollution or the age of the pollutants in the incoming air masses, as
139 increased concentrations of semi-volatile compounds are usually associated with
140 anthropogenic sources, especially in the urban environment (Mahbub et al., 2011, Schnelle-
141 Kreis et al., 2007, Xu and Zhang, 2011). Thus, a high $LDSA_{ratio}$ is expected to be associated
142 with fresher pollution which usually has a higher content of volatile compounds (i.e.,
143 pollution sources at a close distance from the site), while lower ratios are probably
144 associated with either cleaner conditions or more regional and aged pollution with higher
145 concentrations of semi-volatile compounds, generally associated with sources at a greater
146 distance from the measuring site. This specific metric was also used in our previous study
147 (Bousiotis et al., 2021) and the consistency of the results between the two will be
148 compared.

149 For better characterisation of the larger particles, the Aerodyne ACSM was used, providing
150 information about its composition in the size range between 40 nm to 1 μm for NO_3^- , SO_4^{2-}
151 and organic content. For the comparison of the results, data from RG instruments were also
152 used, namely a Palas FIDAS (for PM), a Teledyne T500U (for NO_x), a Thermo 49i (for O_3) and
153 an AE33 aethalometer from Magee Scientific (for BC). Comparison of the regulatory
154 instruments and the LCS allows for consistency of the results between instrument types to
155 be checked. More information about the sensors and instruments used in this study can be
156 found in Bousiotis et al., (2021).

157 Finally, for the present study the PMF analysis was performed using the second iteration of
158 the PMF software developed by Paatero (2004a; 2004b). Data was analysed using the
159 Openair package for R (Carlslaw and Ropkins, 2012), and back trajectory data were
160 extracted by NOAA Air Resources Laboratory and calculated using the HYSPLIT model
161 (Draxler and Hess, 1998).

162

163

164 2.2 Positive Matrix Factorisation



165 The PMF is a multivariate data analysis, developed by Paatero (Paatero and Tapper, 1993;
166 1994), which is the most commonly used method for source apportionment and has been
167 applied numerous times in the field of aerosol science. The method is a weighted least-
168 squares technique that describes relationships among species measurements (Reff et al.,
169 2007). It assumes that X is a matrix of observed data, typically either particle number size
170 distributions (PNSDs) or chemical composition data, and u is the known matrix of the
171 experimental uncertainty of X . Both X and u are of dimensions $n \times m$ (where n is the number
172 of measurements and m is the number of species measured). The method solves the
173 bilinear matrix problem $X = GF + E$ where F is the unknown right hand factor matrix
174 (sources) of dimensions $p \times m$, G is the unknown left hand factor matrix (contributions) of
175 dimensions $n \times p$, and E is the matrix of residuals. The problem is solved in the weighted
176 least-squares sense: G and F are determined so that the Euclidean norm of E divided
177 (element-by-element) by u is minimized. Furthermore, the solution is constrained so that all
178 the elements of G and F are required to be non-negative (Paatero and Tapper, 1994). Higher
179 F values account for better association of the given variable with the factor it is assigned to,
180 while higher G values account for greater contribution of the factor at the given time period.

181 In the present analysis, a combination of both PNSD and particle composition data were
182 used. Such a combination may cause several shortcomings in the application of the PMF as
183 different types of data are used (Beddows and Harrison, 2019). To overcome these
184 shortcomings the two-step PMF method, proposed by Beddows and Harrison (2019), was
185 used. In the first step of the method, a part of the dataset is PMF-analysed (i.e. composition)
186 and a solution is provided. The time series G values (and errors) of the solution from the
187 first step are then used as input variables to the second step, where they are combined with
188 the additional measurements (i.e. PNSD data) dataset applying a second PMF analysis. In
189 the present study the opposite path was considered, with the first step using the PNSD
190 provided by the OPC sensor and the inclusion of particle composition data in the second
191 step. This was explicitly done for two reasons: 1. to test the capabilities of the LCS in source
192 apportionment, 2. to connect specific PNSD profiles with specific pollution sources.
193 Furthermore, on the second step of the analysis detailed in Beddows and Harrison (2019)
194 the explained variance of the factors from the first step were maximised. This directly
195 connects the additional variables in the second step with the PNSD profiles found in the first



196 step, excluding the possible factors formed with the data from the additional LCS data. In
197 the present study, this step in this method was omitted, as the aim is to present the results
198 of the receptor model as they occur in real life using a combination of LCSs measuring both
199 particle number concentrations and composition.

200 For the study site, particle number concentration data were available from the OPC for
201 particles of diameter $< 40 \mu\text{m}$, but only data up to $10 \mu\text{m}$ were used. This was due to the
202 lack of sufficient non-zero counts in the larger size bins above that size threshold, which
203 disfavours PMF analysis to be completed. Additionally, separate LCS data for NO and NO₂
204 were available. The NO data showed sensible variation, however, a great number of the NO
205 data points had low negative values due to their very low concentrations, which is
206 impossible data for the PMF algorithm. Rather than removing the negative numbers or
207 artificially calibrating the data upwards, we use NO_x (NO + NO₂) as the variable of interest.
208 Finally, to avoid the increased uncertainties from the use of unavailable data (as missing
209 data are treated with increased uncertainties), a time window for which all data were
210 available was chosen. Thus, data availability is 100% and no special treatment was
211 considered for missing data.

212

213 **3. Results**

214 **3.1 General conditions at the BAQS site.**

215 The measuring period (16th to 30th of October 2020) was chosen as it is a period which
216 presented rather typical meteorological conditions in the area, had no missing data from
217 any of the instruments used, and because they were the last days before the second
218 lockdown due to COVID-19 was applied (31st of October 2020). General meteorological
219 conditions were rather typical for the period in Birmingham, UK. As a result, the conditions
220 and activities in the surrounding area found in this period are considered almost consistent
221 with the normal conditions at the site in the autumn season. Mean temperature was $10.0 \pm$
222 2.5°C and mean relative humidity was $87.9 \pm 7.5 \%$ (standard deviations are calculated using
223 hourly data) during the measurement period. The average wind profile (Fig. S1) was also
224 typical for the UK with mainly southwestern winds of relatively low speed ($2.1 \pm 1.1 \text{ m s}^{-1}$).

225



226 **3.2 First step PMF analysis (PNSD analysis)**

227 PMF is a descriptive model having no objective criterion in the choice of the optimal number
228 of factors (Paatero et al., 2002). A 4-factor solution was chosen for this analysis. This is due
229 to the relatively limited period analysed as, as mentioned earlier, no significant variation
230 was found in either the meteorological conditions or the sources that affected the air
231 quality in the area. Solutions with additional factors were also attempted but these
232 provided no extra information on additional sources, rather the additional factors separated
233 factors that had already found into smaller groups with no significant covariation. The PNSD
234 profiles of the factors found are presented in Figure S2. Due to the limited variation of the
235 PNSD profiles when presenting all the size bins available, making some of them appear
236 identical (i.e. Factor 2 and 3, due to the increasing particle number concentration as the size
237 decreases), the smallest particle diameter size bin at 400 nm (particle diameter range
238 between 350 to 460 nm) was removed to better present the variation on the larger sizes.
239 Thus, the particle profiles without the smallest available size are presented in Figure 2. The
240 profiles in the range between 500 nm to 10 μm for the four factors, associated with unique
241 formations extracted from the method are:

- 242 • Factor 1, that presents no significant peaks in the measured range of the OPC, but
243 does show a steady increasing trend with particle diameters below 1 μm
- 244 • Factor 2, with a distinct particle diameter peak at about 2 μm
- 245 • Factor 3, with a distinct particle diameter peak at about 2 μm and an increasing
246 trend below 750 nm
- 247 • Factor 4, accounting for particle diameter peaking at about 750 nm and 1.5 μm .

248

249 **3.3 Second step PMF with LCS data (LC analysis)**

250 The four-factor solution was also chosen in the second step analysis, for which the results of
251 the first step are combined with the additional particle and gas phase composition datasets
252 from LCS. The addition of more factors instead of adding information or providing clearer
253 associations with the factors from the first step, it separated the existing factors and their
254 association with the particle composition data into mixed factor groups with less significant
255 contributions of the variables. The association of the variables with each factor is presented
256 in figure 3, while the temporal variation of the contributions G of all the factors from this



257 analysis is presented in figure 4, along with the wind profile for some periods when each
258 factor was dominant.

259

260 The four new factors are:

261 **LC1 (Local and city centre pollution on calm conditions):** The LC1 is strongly associated with
262 the first factor from the initial PMF on the PNSD. For the period when the contribution of
263 this factor is higher (18th and 19th of October, see fig. 4) rather slow winds prevail from
264 many sectors (in this case mainly from the southwest). This factor has higher contributions
265 during calm conditions and during periods with north-eastern winds, though with lower
266 contribution (Fig. 5). It is highlighted that at the northeast of the specific site is the city
267 centre of Birmingham which is one of the main sources of pollution as found from a
268 previous study (Bousiotis et al., 2021). Looking at the diurnal variation (Fig. S3) of this factor
269 we see increased contributions during early morning and evening hours, likely associating it
270 with the morning and evening rush hours. The increased contributions during night-time
271 should not be overlooked and are probably the result of the lower boundary layer height
272 (BLH) during this time of the day. Additional data analysis shows an increased association of
273 this factor with PM₁ (Fig. 3), though this association is reduced for particles of larger sizes,
274 further confirming the lack of additional peaks on greater sizes. This along with the
275 increased association with the LDSA indicates the presence of large number of particles
276 below the detection limit of the instrument. This factor is also associated with almost all the
277 pollutants used, such as NO_x, CO and BC, though not as strongly as factor LC3 that is
278 discussed below, probably associated with pollution sources in a closer range to the
279 measuring station, as well as to a smaller extent with pollution from the city centre. Its
280 connection with air masses from the northeast is also confirmed from the back trajectory
281 analysis (Fig. 6), in which the highest contributions of this factor were found for air masses
282 from the northeast.

283 **LC2 (Marine):** This factor is strongly associated with the fourth PNSD factor from the initial
284 analysis (fig. 3). It presents relatively high association with PM which increases as the size
285 increases. No other significant association is found rather than relatively weak ones with
286 ozone, CO and the LDSA_{ratio}. It does not have a clear diurnal variation (fig. S3), though it has
287 slightly increased contributions during night-time. Higher contributions for this factor are
288 found with south and south-eastern winds of high speed (fig. 4 and 5). This can be seen in



289 Figure 4, where the highest contributions of this factor are associated with strong southern
290 winds. The marine nature of this factor is clearly highlighted through the back trajectory
291 analysis for this factor (Fig. 6) in which higher contributions are mostly found with air
292 masses originating from the north Atlantic Ocean, while some contributions from southern
293 Spain and Africa, which may be associated with Saharan dust and pollution from these
294 areas.

295 **LC3 (midday city centre and southwest pollution):** This factor does not have any significant
296 association with any of the factors from the PMF analysis of the PNSD (fig. 3). It presents
297 greater contributions during the midday (fig. S3), and it is associated with north-eastern and
298 southwestern winds (fig. 5). It has high contributions with all the pollutants included in the
299 analysis and the $LDSA_{ratio}$, which points to fresher pollution (pollution sources closer to the
300 measuring station). Such sources of pollution in most cases are associated with particles of
301 sizes smaller than that measured by the OPC, hence the lack of association with any of the
302 factors found from the PNSD analysis. The back trajectory analysis provides no clear origin
303 for the air masses of this factor (fig. 6), which may indicate a relatively smaller pollution
304 lifetime, which is associated with incoming air masses from all directions.

305 **LC4 (Urban background):** This factor has a rather strong association with the second factor
306 from the PNSD analysis and a weaker one with the third one (Fig. 3). It does not have a clear
307 diurnal variation (fig. S3) and it is mainly associated with north-eastern winds (Fig. 5). It
308 presents weak associations with all the variables inputted in the PMF analysis making it hard
309 to distinguish either a source or conditions for which this factor is enhanced. The back
310 trajectory analysis though shows that this factor is associated with air masses from
311 continental Europe as well as Scandinavia (Fig. 6), which for the UK, usually contain aged
312 and hence typically larger secondary PM pollutants.

313

314 **3.4 Second step PMF with RG data (RG analysis)**

315 While the primary aim of the present study is to highlight the capabilities of LCS in source
316 apportionment, the measurements provided by these devices are mainly focused on gas
317 phase pollutants which are in most cases associated solely with ultrafine particles. The OPC
318 measurements used for this site have a particle diameter range between 400 nm to 10 μ m.
319 Thus, apart from using data from RG instruments measuring gas phase pollutants, it was



320 considered sensible to add data from an ACSM, which measures compounds associated with
321 larger particles, such as nitrate, sulphate, and organic compounds (used in this analysis).
322 Some of the factors in this analysis are rather similar with those formed from the analysis
323 using LCS dataset. Thus, the **RG1** factor in this analysis is mainly associated with the first
324 factor from the PNSD analysis in the first step (Fig. 7), similar to that found also in LC1 (Fig.
325 3). The wind conditions are also similar for which these factors from the two analyses
326 present their highest contribution (Fig. 8), as well as their temporal variation (Fig. S4) and
327 diurnal variation (Fig. S5). The additional information granted using the ACSM data is the
328 strong association of this factor with nitrate, and a stronger association with NO_x and BC are
329 also found, compared to the LC analysis. This further associates this factor with nearby
330 sources of pollution which prevail with low wind speeds and may associate the conditions of
331 this factor with the low BLH height found during that time, though high contributions were
332 also found for early morning and evening hours, as in the LC analysis for the similar factor.
333 Finally, the back trajectory analysis (fig. 9) shows higher contributions associated with air
334 masses from the northeast, further confirming its similarity with the first factor from the LC
335 analysis and its urban origins.

336 The **RG2** is unique and has no association with the factors from the PMF on PNSD data and
337 is strongly associated only with sulphate (Fig. 7). It does not have a clear diurnal variation
338 (fig. S5) and seems to have higher contributions with southwestern winds of rather high
339 speed and to a lesser extent with north-easterly winds (Fig. 8). The back trajectory analysis
340 (Fig. 9), while presenting few relatively high contributions from continental Europe, mainly
341 associates this factor with incoming air masses from all sea origins surrounding the UK. This
342 is expected as the ocean is a source of sulphate containing compounds (for the particles at
343 the size range measured by the OPC), either sea-salt sulphate or marine biogenic sulphate
344 (Lin et al., 2012; Raes et al., 2000).

345 The **RG3** is similar to the LC2 and is mainly associated with the fourth factor from the PNSD
346 analysis and to a lesser extent with the third (Fig. 7). This factor has slightly increased
347 contributions during night-time (Fig. S5) and south and southwestern winds (Fig. 8). It
348 presents increased associations with increasing PM size, though in this case it is also
349 strongly associated with O₃. Unfortunately, no Cl or Na data were available to further
350 determine the marine nature of this factor. The back trajectory analysis though once again
351 presents higher contributions with marine air masses (Fig. 9), though some hot spots are



352 also found from continental Europe, which probably explain to an extent the small
353 associations found with NO_x and organic compounds from the ACSM.
354 Finally, the **RG4** is mainly associated with the second factor and to a lesser extent with the
355 third from the PNSD analysis (Fig. 7). It presents higher contributions with north-eastern
356 winds (Fig. 8), has an unclear diurnal variation (Fig. S5), and presents higher contributions
357 with air masses from continental Europe (Fig. 9), like the LC4 from the second-step analysis.
358 While in that analysis it was difficult to characterise the sources for that factor, the strong
359 association with organic compounds found here with the addition of the ACSM data helps in
360 its clearer characterisation.

361

362 **4. Discussion**

363 **4.1 Comparison of the results from the second-step analysis**

364 It should be noted that regardless of any possible similarities between the two (second-
365 step) analyses, a direct comparison of the results should be conducted with great care. As
366 different variables are considered, even minor differences may result in different trends,
367 contribution of variables and the sources described. Regardless, the results of the two
368 analyses have great similarities especially on specific factors that are associated with the
369 same particle size distribution profiles (from the PNSD analysis), contribution of chemical
370 compounds and diurnal variation. Three factors were found to have great similarities and
371 were associated with similar particle profiles. Specifically, these are the factors describing
372 the sources of particles which are either in close proximity to the measuring station or occur
373 with almost calm conditions (Factor 1 on both analyses), the marine factor (Factor 2 on LC
374 analysis and 3 on RG analysis) and the continental factor (Factor 4 on both analyses).
375 Looking at their temporal contributions (Fig. 4 and S4), the first factors on both analyses
376 appear to consistently peak on periods when the second set of factors (LC2 and RG3)
377 presents lower G contributions (and vice versa), which is expected due to the nature of their
378 sources. The factors on both sets though have almost identical temporal variation of their G
379 contributions regardless of the dataset. For the fourth factors on both analyses, though
380 presenting similar associations with their variables, differences are found in their temporal
381 variations with the addition of the ACSM data. This shows that while these factors appear to
382 be almost identical, small differences can still be found in their temporal variation and



383 variable associations, when different datasets are considered. Nevertheless, the addition of
384 the ACSM data shows a very high contribution of NO_3^- on the first RG factor, SO_4^{2-} for the
385 second factor and the organic component on the fourth factor.

386 The remaining factor from both analyses though is completely different between the two
387 analyses and point towards the differences on the variables used for each. In the LC analysis
388 the factor formed consists of sources that are associated with fresher pollution sources.

389 Thus, a factor with strong associations with all the pollutants available was formed, it was
390 not associated with any of the PNSD formations from the first-step analysis and presented a
391 unique diurnal variation peaking midday. This should be expected as the particle size

392 measured by the OPC is much larger compared to the size of the particles these chemical
393 compounds are usually associated with. The occurrence of this factor was probably included
394 partially to the first and fourth factor of the RG analysis, as these present relatively higher
395 associations with NO_x and BC and more enhanced contributions during midday hours

396 compared to their LC analysis counterparts.

397 Finally, using the RG instrument data, the additional factor is associated with sulphate
398 alone. This is a result that was consistent regardless of the number of factors used, either
399 greater or smaller. Sulphate containing compounds have a lower volatility compared to the
400 other chemical compounds used in the analysis and is relatively more stable with a rather
401 small seasonal variation (Utsunomiya and Wakamatsu, 1996), thus having a longer lifespan
402 and distance of travel. As a result, sulphate was found not to be associated with any other
403 chemical compound and always formed a factor of its own (regardless of the number of
404 factors chosen).

405

406 **4.2 Comparison with the results from a previous study.**

407 Although different methodologies were used with the previous analysis for the BAQS site
408 (Bousiotis et al., 2021), as well as for different time periods, many similarities were found
409 for the sources of particles at the site. The main source of smaller particles at the site in the
410 previous analysis is found to be the city centre in the northeast, for which relatively high
411 concentrations of NO_x were found. Similar is the case in the present analysis, as for the
412 sources found to be associated with north-easterly winds an association was also found with
413 NO_x and the $\text{LDSA}_{\text{ratio}}$. Additionally, a source of sulphate found with southerly winds was also



414 confirmed in the present study, with the association of high sulphate concentrations with a
415 factor, which presents higher contributions with winds from the southern sector. While in
416 the previous analysis the sources responsible for this source could not be pinpointed, in the
417 present analysis, using a back trajectory analysis, the sulphate factor was associated with
418 marine particle sources from all directions. Furthermore, a factor in the present analysis,
419 which identifies hot spots south of the measuring station with strong presence of PM of all
420 sizes, was also found with the k-means analysis in the previous study, though in that case it
421 was more associated with the pollution sources from that side rather than the long-range
422 transport found here.

423 These similarities are very encouraging, as even though the analyses were made for
424 different periods and using different methods, there is consistency between the results. This
425 means that regardless of the different seasons studied (previous analysis was performed
426 during winter to early spring), the sources of particles (and pollution) are relatively uniform,
427 without significant changes.

428 Additionally, the k-means method identified sets of conditions that either promote or
429 suppress the pollution at the sites (as this can be illustrated with the variable particle
430 concentrations between the clusters found from the analysis), rather than separate sources
431 of pollution that affect the site. While this provides a more realistic picture of the conditions
432 it makes it harder to distinguish the specific sources and their effect in its air quality. On the
433 other hand, the PMF not only provides clearer separation of the sources, but the temporal
434 contribution of each source as well, which shows the real extent of the effect of each source
435 of particles or pollutants, thus achieving source apportionment rather than just the
436 identification of pollution sources that the k-means offers. The k-means approach identifies
437 the effect of the sources of particles, but it also separates cleaner periods as separate
438 clusters. These two effects gives a more complete overall picture of the air quality at a site.
439 PMF could also provide this information, but it would be more difficult to obtain looking at
440 the different sources and the conditions that keep them to low contributions (this would
441 also require a much greater number of factors).

442 Furthermore, due to the complexity of the clusters from the k-means, pinpointing the
443 sources that the particles are associated with is difficult. This is due to the clusters, being a
444 set of different sources and conditions rather than clearly separated sources, were not
445 clearly associated with distinct wind directions, speeds or hot-spots. Contrary to that, the



446 factors formed by the PMF present clearer association with specific sectors, thus making it
447 easier to define the sources associated with them, as in the results they are presented as
448 hot spots within the polar plots.

449 The analysis of atmospheric data using either k-means or PMF are proven to provide
450 adequate and trustworthy information for the sources of particles and by extension of
451 pollution at a site, even with the sole use of LCS as shown in this paper and the preceding
452 Bousiotis et al. 2021 paper. The combined use of both approaches provides a clearer picture
453 of the different sources and their effect, as the PMF is able to better separate and provide
454 the effect of the sources of pollution that affect the air quality at a site and the k-means
455 provides a more realistic representation of the conditions at a site, by showing the
456 combined effect of these sources. The relative consistency of the results found between the
457 two analyses, even being in different time periods, is very encouraging and shows that the
458 very important information of pollution receptor modelling is viable with LCS, providing a
459 much-needed alternative for countries or scenarios where the use of regulatory-grade
460 instruments is not feasible. The significantly lower price point of LCSs means that in addition
461 to hyperlocal measurement of air pollution, it should now be possible to deliver hyperlocal
462 source apportionment of air pollution. This ability will open new research and industrial
463 abilities to pinpoint air pollution sources and subsequently manage them.
464 Finally, the $LDSA_{ratio}$, a variable that was introduced in the previous analysis, was included in
465 the present one as well. As in the previous analysis, this ratio was found to be more
466 associated with fresher pollution from combustion sources near to the measuring station,
467 for which it has reliably performed in both analyses.

468

469 **5. Conclusions**

470 To solve air quality problems and to deliver the associated policy making effectively, it is
471 vital to have a methodology to measure the sources of air pollution, and their relative
472 importance. Historically, this has been achieved using expensive RG instruments. The cost
473 implications of these studies make assessment at dense spatial resolutions limited. In this
474 study, data from a low-cost OPC and other LCS, measuring gas phase pollutants, black
475 carbon and the lung deposited surface area of particles in BAQS were analysed using the
476 two-step PMF analysis. Four factors were formed from this analysis and were associated



477 with their respective sources and to a great extent with unique PNSD profiles. The following
478 factors were found: a factor associated with either combustion sources in close proximity of
479 the measurement site or associated with calm conditions, a marine factor, a factor
480 associated with midday activities from the city centre and a more constant factor from the
481 northeast. The same analysis was also performed using data from RG instruments and the
482 same PNSD factors. This was done to evaluate the results from the low-cost sensor analysis,
483 as well as to further characterise and clarify the sources associated with the factors formed.
484 Significant agreement was found between the results of the two analyses, highlighting that
485 the LCS are capable for carrying out such analyses. The additional ACSM data from the
486 second analysis further helped in the characterisation of the composition of the particles of
487 each factor, clarifying the sources associated with nitrate, sulphate and organic compounds
488 at the site, as well as strongly associating some with unique PNSD profiles. While in their
489 present state, the LCSs do not possess the full capability of the RG instruments for providing
490 high accuracy measurements, considering the limitations they were found to be adequate in
491 providing with the trends of the particles and pollutants measured which are important for
492 source apportionment studies. This is done at a fraction of the equipment cost; see
493 Bousiotis et al. 2021 for cost estimates.

494 Furthermore, comparing the results from the PMF to those from the k-means analysis
495 showed the different strengths and weaknesses of each approach. The PMF is better in
496 pinpointing the effect of separate sources of pollution, but it is difficult to give a clear
497 representation of the actual conditions when each factor affects the site. The k-means is not
498 as efficient in clearly separating the different sources, but it does provide a more realistic
499 picture of the air quality at a site in relation to the ambient conditions. The combined use of
500 both methods though provided a clearer picture for the conditions at the site.

501 The methodologies developed and used in this study will help to reliably facilitate source
502 apportionment studies in the future, with either the sole use of LCS or their combination
503 with RG instruments. As for a given site, specific PNSD formations are associated with
504 specific conditions and sources (Harrison et al., 2011), by creating a repository of unique
505 PNSDs at a site and associating them with their respective sources, in the future the source
506 apportionment may be done to an extent using only PNSD profiles and meteorological data
507 alone. This will do much in simplifying the source apportionment process allowing its wider
508 application and help in dealing with environmental challenges. For this though, further



509 testing in more diverse environments and scenarios is needed which, along with the
510 anticipated development of the LCS, will provide a denser and reliable measuring network
511 even for countries with lower incomes and help for cleaner and healthier environmental
512 conditions.

513

514

515 **Author Contributions**

516 The study was conceived and planned by FDP who also contributed to the final manuscript,
517 and DB who carried out the analysis and prepared the first draft. AS, MH, DCSB and SD
518 provided data for the analysis. DCSB provided help with the analysis of the data. RMH, PME
519 and AB contributed to the final manuscript.

520

521 **Competing Interests**

522 The authors have no conflict of interests.

523

524 **Acknowledgements**

525 We thank the OSCA team (Integrated Research Observation System for Clean Air) at the
526 Birmingham Air Quality Supersite (BAQS), funded by NERC (NE/T001909/1), for help in data
527 collection for the regulatory-grade instruments. We thank Lee Chapman for access to his
528 meteorological dataset used in the analysis.

529 **Financial support.**

530 This research has been supported by the Natural Environment Research Council (NERC grant
531 no. NE/T001879/1), the Engineering and Physical Sciences Research Council (EPSRC grant
532 no. EP/T030100/1) and internal EPSRC funding provided to the University of Birmingham for
533 Impact Acceleration.

534

535



536 **References**

537

538 Austin, E., Novosselov, I., Seto, E. and Yost, M. G.: Laboratory evaluation of the Shinyei
539 PPD42NS low-cost particulate matter sensor, *PLoS One*, 10(9), 1–17,
540 doi:10.1371/journal.pone.0137789, 2015.

541

542 Beddows, D. C. S., Harrison, R. M., Green, D. C. and Fuller, G. W.: Receptor modelling of both
543 particle composition and size distribution from a background site in London, UK, *Atmos.*
544 *Chem. Phys.*, 15(17), 10107–10125, doi:10.5194/acp-15-10107-2015, 2015.

545

546 Beddows, D.C.S., and Harrison, R.M.: Receptor modelling of both particle composition and
547 size distribution from a background site in London, UK – a two-step approach, *Atmos. Chem.*
548 *Phys.*, 19, 39 – 55, <https://doi.org/10.5194/acp-19-39-2019>, 2019.

549

550 Bousiotis, D., Pope, F.D., Beddows, D.C.S., Dall'Osto, M., Massling, A., Nøjgaard, J.K.,
551 Nordstrøm, C., Niemi, J.V., Portin, H., Petäjä, T., Perez, N., Alastuey, A., Querol, X.,
552 Kouvarakis, G., Mihalopoulos, N., Vratolis, S., Eleftheriadis, K., Wiedensohler A., Weinhold,
553 A., Merkel, M., Tuch, T. and Harrison R.M.: A phenomenology of new particle formation
554 (NPF) at 13 European sites, *Atmos. Chem. Phys.*, 21, 11905 - 11925,
555 <https://doi.org/10.5194/acp-21-11905-2021> 2021.

556 Bousiotis, D., Singh, A., Haugen, M., Beddows, D.C.S., Diez, S., Edwards, P.M., Boies, A.,
557 Harrison, R.M. and Pope, F.D.: Assessing the sources of particles at an urban background site
558 using both regulatory grade instruments and low-cost sensors – A comparative study,
559 *Atmos. Meas. Tech.*, 14, 4139 – 4155, <https://doi.org/10.5194/amt-14-4139-2021>, 2021.

560

561 Carslaw, D. C. and Ropkins, K.: openair — An R package for air quality data analysis, *Environ.*
562 *Model. Softw.*, 27–28, 52–61, doi:10.1016/j.envsoft.2011.09.008, 2012.

563

564 Crilley, L. R., Shaw, M., Pound, R., Kramer, L. J., Price, R., Young, S., Lewis, A. C., and Pope, F.
565 D.: Evaluation of a low-cost optical particle counter (Alphasense OPC-N2) for ambient air



- 566 monitoring, *Atmos. Meas. Tech.*, 11, 709–720, <https://doi.org/10.5194/amt-11-709-2018>,
567 2018.
- 568
- 569 Crilley, L. R., Singh, A., Kramer, L. J., Shaw, M. D., Alam, M. S., Apte, J. S., Bloss, W. J.,
570 Hildebrandt Ruiz, L., Fu, P., Fu, W., Gani, S., Gatari, M., Ilyinskaya, E., Lewis, A. C., Ng'ang'a,
571 D., Sun, Y., Whitty, R. C. W., Yue, S., Young, S. and Pope, F. D.: Effect of aerosol composition
572 on the performance of low-cost optical particle counter correction factors, *Atmos. Meas.*
573 *Tech.*, 13(3), 1181–1193, doi:10.5194/amt-13-1181-2020, 2020.
- 574
- 575 Draxler, R. R. and Hess, G. D.: An Overview of the HYSPLIT_4 Modelling System for
576 Trajectories, Dispersion, and Deposition, *Aust. Meteorol. Mag.*, 47(January), 295–308, 1998.
- 577
- 578 De Vito, S., Esposito, E., Castell, N., Schneider, P. and Bartonova, A.: On the robustness of
579 field calibration for smart air quality monitors, *Sensors Actuators, B Chem.*, 310(July 2019),
580 127869, doi:10.1016/j.snb.2020.127869, 2020.
- 581
- 582 Feinberg, S. N., Williams, R., Hagler, G., Low, J., Smith, L., Brown, R., Garver, D., Davis, M.,
583 Morton, M., Schaefer, J. and Campbell, J.: Examining spatiotemporal variability of urban
584 particulate matter and application of high-time resolution data from a network of low-cost
585 air pollution sensors, *Atmos. Environ.*, 213(May), 579–584,
586 doi:10.1016/j.atmosenv.2019.06.026, 2019.
- 587 Giordano, M.R., Malings, C., Pandis, S.N., Presto, A.A., McNeill, V.F., Westervelt, D.M.,
588 Beekmann, M., and Subramanian, R.: From low-cost sensors to high-quality data: A
589 summary of challenges and best practices for effectively calibrating low-cost particulate
590 matter mass sensors, *Journal of Aerosol Science*,
591 <https://doi.org/10.1016/j.jaerosci.2021.105833>, 2021.
- 592 Hagan, D. H., Gani, S., Bhandari, S., Patel, K., Habib, G., Apte, J. S., Hildebrandt Ruiz, L. and
593 Kroll, J. H.: Inferring Aerosol Sources from Low-Cost Air Quality Sensor Measurements: A
594 Case Study in Delhi, India, *Environ. Sci. Technol. Lett.*, 6(8), 467–472,
595 doi:10.1021/acs.estlett.9b00393, 2019.



- 596
- 597 Hagan, D. and Kroll, J.: Assessing the accuracy of low-cost optical particle sensors using a
598 physics-based approach, *Atmos. Meas. Tech. Discuss.*, 1–36, doi:10.5194/amt-2020-188,
599 2020.
- 600
- 601 Harrison, R. M., Beddows, D. C. S. and Dall'Osto, M.: PMF analysis of wide-range particle size
602 spectra collected on a major highway, *Environ. Sci. Technol.*, 45(13), 5522–5528,
603 doi:10.1021/es2006622, 2011.
- 604
- 605 Haugen, M.J., Singh, A., Bousiotis, D., Pope, F.D., Boies, A.M.: Demonstrating the ability to
606 differentiate between semi-volatile and solid particle events with low-cost lung-deposited
607 surface area and black carbon particle sensors, *Atmosphere*, in submission, 2022.
- 608
- 609 Hopke, P. K.: Review of receptor modeling methods for source apportionment, *J. Air Waste*
610 *Manag. Assoc.*, 66(3), 237–259, doi:10.1080/10962247.2016.1140693, 2016.
- 611
- 612 Jovašević-Stojanović, M., Bartonova, A., Topalović, D., Lazović, I., Pokrić, B. and Ristovski, Z.:
613 On the use of small and cheaper sensors and devices for indicative citizen-based monitoring
614 of respirable particulate matter, *Environ. Pollut.*, 206, 696–704,
615 doi:10.1016/j.envpol.2015.08.035, 2015.
- 616
- 617 Kan, H., Chen, B. and Hong, C.: Health impact of outdoor air pollution in China: Current
618 knowledge and future research needs, *Environ. Health Perspect.*, 117(5), 12737,
619 doi:10.1289/ehp.12737, 2009.
- 620
- 621 Kanaroglou, P. S., Jerrett, M., Morrison, J., Beckerman, B., Arain, M. A., Gilbert, N. L. and
622 Brook, J. R.: Establishing an air pollution monitoring network for intra-urban population
623 exposure assessment: A location-allocation approach, *Atmos. Environ.*, 39(13), 2399–2409,
624 doi:10.1016/j.atmosenv.2004.06.049, 2005.
- 625
- 626 Kosmopoulos, G., Salamalikis, V., Pandis, S. N., Yannopoulos, P., Bloutsos, A. A. and
627 Kazantzidis, A.: Low-cost sensors for measuring airborne particulate matter: Field evaluation



- 628 and calibration at a South-Eastern European site, *Sci. Total Environ.*, 748(October), 141396,
629 doi:10.1016/j.scitotenv.2020.141396, 2020.
- 630
- 631 Krause, A., Zhao, J. and Birmili, W.: Low-cost sensors and indoor air quality: A test study in
632 three residential homes in Berlin, Germany, *Gefahrstoffe Reinhaltung der Luft*, 79(3), 87–94,
633 doi:10.37544/0949-8036-2019-03-49, 2019.
- 634
- 635 Leoni, C., Pokorná, P., Hovorka, J., Masiol, M., Topinka, J., Zhao, Y., Křůmal, K., Cliff, S.,
636 Mikuška, P. and Hopke, P. K.: Source apportionment of aerosol particles at a European air
637 pollution hot spot using particle number size distributions and chemical composition,
638 *Environ. Pollut.*, 234, 145–154, doi:10.1016/j.envpol.2017.10.097, 2018.
- 639
- 640 Lepistö, T., Kuuluvainen, H., Lintusaari, H., Kuittinen, N., Salo, L., Helin, A., Niemi, J.V.,
641 Manninen, H.E., Timonen, H., Jalava, P., Saarikoski, S. and Rönkkö, T.: Connection between
642 lung deposited surface area (LDSA) and black carbon (BC) concentrations in road traffic and
643 harbour environments, *Atmospheric Environment*, 272, 118931,
644 <https://doi.org/10.1016/j.atmosenv.2021.118931>, 2022.
- 645
- 646 Lewis, A. C., von Schneidmesser, E., Peltier, R. E., Lung, C., Jones, R., Zellweger, C.,
647 Karppinen, A., Penza, M., Dye, T., Hüglin, C., Ning, Z., Leigh, R., Hagan, D. H., Laurent, O. and
648 Carmichael, G.: Low-cost sensors for the measurement of atmospheric composition:
649 overview of topic and future applications. [online] Available from:
650 http://www.wmo.int/pages/prog/arep/gaw/documents/Draft_low_cost_sensors.pdf, 2018.
- 651
- 652 Liang, Y., Wu, C., Jiang, S., Li, Y. J., Wu, D., Li, M., Cheng, P., Yang, W., Cheng, C., Li, L., Deng,
653 T., Sun, J. Y., He, G., Liu, B., Yao, T., Wu, M. and Zhou, Z.: Field comparison of
654 electrochemical gas sensor data correction algorithms for ambient air measurements,
655 *Sensors Actuators, B Chem.*, 327(November 2020), doi:10.1016/j.snb.2020.128897, 2021.
- 656
- 657 Lin, C. T., Baker, A. R., Jickells, T. D., Kelly, S. and Lesworth, T.: An assessment of the
658 significance of sulphate sources over the Atlantic Ocean based on sulphur isotope data,
659 *Atmos. Environ.*, 62, 615–621, doi:10.1016/j.atmosenv.2012.08.052, 2012.



- 660
- 661 Mahbub, P., Ayoko, G.A., Goonetilleke, A., Egodawatta, P.: Analysis of the build-up of semi
662 and non volatile organic compounds on urban roads, *Water Res.* 45(9), 2835 - 2844, doi:
663 10.1016/j.watres.2011.02.033, 2011.
- 664
- 665 Manisalidis, I., Stavropoulou, E., Stavropoulos, A. and Bezirtzoglou, E.: Environmental and
666 Health Impacts of Air Pollution: A Review, *Front. Public Heal.*, 8(February), 1–13,
667 doi:10.3389/fpubh.2020.00014, 2020.
- 668
- 669 Mannucci, P. M. and Franchini, M.: Health effects of ambient air pollution in developing
670 countries, *Int. J. Environ. Res. Public Health*, 14(9), 1–8, doi:10.3390/ijerph14091048, 2017.
- 671
- 672 Miskell, G., Salmond, J. A. and Williams, D. E.: Use of a handheld low-cost sensor to explore
673 the effect of urban design features on local-scale spatial and temporal air quality variability,
674 *Sci. Total Environ.*, 619–620, 480–490, doi:10.1016/j.scitotenv.2017.11.024, 2018.
- 675
- 676 Moore, F. C.: Climate change and air pollution: Exploring the synergies and potential for
677 mitigation in industrializing countries, *Sustainability*, 1(1), 43–54, doi:10.3390/su1010043,
678 2009.
- 679
- 680 Nagendra, S., Reddy Yasa, P., Narayana, M., Khadirnaikar, S. and Pooja Rani: Mobile
681 monitoring of air pollution using low cost sensors to visualize spatio-temporal variation of
682 pollutants at urban hotspots, *Sustain. Cities Soc.*, 44(September 2018), 520–535,
683 doi:10.1016/j.scs.2018.10.006, 2019.
- 684
- 685 Omokungbe, O. R., Fawole, O. G., Owoade, O. K., Popoola, O. A. M., Jones, R. L., Olise, F. S.,
686 Ayoola, M. A., Abiodun, P. O., Toyeye, A. B., Olufemi, A. P., Sunmonu, L. A. and Abiye, O. E.:
687 Analysis of the variability of airborne particulate matter with prevailing meteorological
688 conditions across a semi-urban environment using a network of low-cost air quality sensors,
689 *Heliyon*, 6(6), e04207, doi:10.1016/j.heliyon.2020.e04207, 2020.
- 690
- 691 Paatero, P. and Tapper, U.: Analysis of different modes of factor analysis as least squares fit



692 problems, *Chemom. Intell. Lab. Syst.*, 18(2), 183–194, doi:10.1016/0169-7439(93)80055-M,
693 1993.
694
695 Paatero, P. and Tapper, U.: Positive Matrix Factorization : A Non-negative factor model with
696 optimal utilization of error estimates of data values, *Environmetrics*, 5(April 1993), 111–126,
697 1994.
698
699 Paatero, P., Hopke, P. K., Song, X.-H., and Ramadan, Z.: Understanding and controlling
700 rotations in factor analytic models, *Chemometr. Intell. Lab.*, 60, 253–264, 2002.
701
702 Paatero P.: User’s guide for positive matrix factorization programs PMF2 and PMF3, Part1:
703 tutorial. University of Helsinki, Helsinki, Finland, 2004a.
704
705 Paatero P.: User’s guide for positive matrix factorization programs PMF2 and PMF3, Part2:
706 references. University of Helsinki, Helsinki, Finland, 2004b.
707
708 Pascal, M., Corso, M., Chanel, O., Declercq, C., Badaloni, C., Cesaroni, G., Henschel, S.,
709 Meister, K., Haluza, D., Martin-Olmedo, P. and Medina, S.: Assessing the public health
710 impacts of urban air pollution in 25 European cities: Results of the Aphekom project, *Sci.*
711 *Total Environ.*, 449(2007105), 390–400, doi:10.1016/j.scitotenv.2013.01.077, 2013.
712
713 Penza, M.: Low-cost sensors for outdoor air quality monitoring, Elsevier Inc., 2019.
714 Petkova, E. P., Jack, D. W., Volavka-Close, N. H. and Kinney, P. L.: Particulate matter
715 pollution in African cities, *Air Qual. Atmos. Heal.*, 6(3), 603–614, doi:10.1007/s11869-013-
716 0199-6, 2013.
717
718 Pokorná, P., Hovorka, J. and Hopke, P. K.: Elemental composition and source identification
719 of very fine aerosol particles in a European air pollution hot-spot, *Atmos. Pollut. Res.*, 7(4),
720 671–679, doi:10.1016/j.apr.2016.03.001, 2016.
721
722 Pope, F. D., Gatari, M., Ng’ang’a, D., Poynter, A. and Blake, R.: Airborne particulate matter
723 monitoring in Kenya using calibrated low cost sensors, *Atmos. Chem. Phys. Discuss.*, 1–31,



- 724 doi:10.5194/acp-2018-327, 2018.
725
- 726 Popoola, O. A. M., Carruthers, D., Lad, C., Bright, V. B., Mead, M. I., Stettler, M. E. J., Saffell,
727 J. R. and Jones, R. L.: Use of networks of low cost air quality sensors to quantify air quality in
728 urban settings, *Atmos. Environ.*, 194(February), 58–70,
729 doi:10.1016/j.atmosenv.2018.09.030, 2018.
730
- 731 Prakash, J., Choudhary, S., Raliya, R., Chadha, T., Fang, J., George, M. P. and Biswas, P.:
732 Deployment of Networked Low-Cost Sensors and Comparison to Real-Time Stationary
733 Monitors in New Delhi, *J. Air Waste Manage. Assoc.*, 0(0),
734 doi:10.1080/10962247.2021.1890276, 2021.
735
- 736 Raes, F., Dingenen, R. Van, Elisabetta, V., Wilson, J., Putaud, J. P., Seinfeld, J. H. and Adams,
737 P.: Formation and cycling of aerosols in the global troposphere, *Atmos. Environ.*, 34, 4215–
738 4240, 2000.
739
- 740 Reff, A., Eberly, S. I. and Bhawe, P. V.: Receptor Modeling of Ambient Particulate Matter Data
741 Using Positive Matrix Factorization: Review of Existing Methods, *J. Air Waste Manage.*
742 *Assoc.*, 57(2), 146–154, doi:10.1080/10473289.2007.10465319, 2007.
743
- 744 Rivas, I., Vicens, L., Basagaña, X., Tobías, A., Katsouyanni, K., Walton, H., Hüglin, C., Alastuey,
745 A., Kulmala, M., Harrison, R. M., Pekkanen, J., Querol, X., Sunyer, J. and Kelly, F. J.:
746 Associations between sources of particle number and mortality in four European cities,
747 *Environ. Int.*, 155(May), doi:10.1016/j.envint.2021.106662, 2021.
748
- 749 Schneider, P., Castell, N., Vogt, M., Dauge, F. R., Lahoz, W. A. and Bartonova, A.: Mapping
750 urban air quality in near real-time using observations from low-cost sensors and model
751 information, *Environ. Int.*, 106(May), 234–247, doi:10.1016/j.envint.2017.05.005, 2017.
752
- 753 Schnelle-Kreis, J., Sklorz, M., Orasche, J., Stölzel, M., Peters, A. and Zimmermann, R.: Semi
754 volatile organic compounds in ambient PM_{2.5}. Seasonal trends and daily resolved source
755 contributions, *Environ. Sci. Technol.*, 41(11), 3821–3828, doi:10.1021/es060666e, 2007.



756

757 Shafran-Nathan, R., Etzion, Y., Zivan, O. and Broday, D. M.: Estimating the spatial variability
758 of fine particles at the neighborhood scale using a distributed network of particle sensors,
759 *Atmos. Environ.*, 218(April), 117011, doi:10.1016/j.atmosenv.2019.117011, 2019.

760

761 Shindler, L.: Development of a low-cost sensing platform for air quality monitoring:
762 application in the city of Rome, *Environ. Technol. (United Kingdom)*, 42(4), 618–631,
763 doi:10.1080/09593330.2019.1640290, 2021.

764

765 Shiraiwa, M., Ueda, K., Pozzer, A., Lammel, G., Kampf, C. J., Fushimi, A., Enami, S., Arangio,
766 A. M., Fröhlich-Nowoisky, J., Fujitani, Y., Furuyama, A., Lakey, P. S. J., Lelieveld, J., Lucas, K.,
767 Morino, Y., Pöschl, U., Takahama, S., Takami, A., Tong, H., Weber, B., Yoshino, A. and Sato,
768 K.: Aerosol Health Effects from Molecular to Global Scales, *Environ. Sci. Technol.*, 51(23),
769 13545–13567, doi:10.1021/acs.est.7b04417, 2017.

770

771 Smith, K. R., Edwards, P. M., Ivatt, P. D., Lee, J. D., Squires, F., Dai, C., Peltier, R. E., Evans, M.
772 J., Sun, Y., and Lewis, A. C.: An improved low-power measurement of ambient NO₂ and O₃
773 combining electrochemical sensor clusters and machine learning, *Atmos. Meas. Tech.*, 12,
774 1325–1336, doi:10.5194/amt-12-1325-2019, 2019.

775

776 Sousan, S., Koehler, K., Thomas, G., Park, J. H., Hillman, M., Halterman, A. and Peters, T. M.:
777 Inter-comparison of low cost sensors for measuring the mass concentration of occupational
778 aerosols, *Aerosol Sci. Technol.*, 50(5), 462–473, doi:10.1080/02786826.2016.1162901, 2016.

779

780 Utsunomiya, A. and Wakamatsu, S.: Temperature and humidity dependence on aerosol
781 composition in the northern Kyushu, Japan, *Atmos. Environ.*, 30(13), 2379–2386,
782 doi:10.1016/1352-2310(95)00350-9, 1996.

783

784 Vajs, I., Drajić, D., Gligorić, N., Radovanović, I. and Popović, I.: Developing relative humidity
785 and temperature corrections for low-cost sensors using machine learning, *Sensors*, 21(10),
786 doi:10.3390/s21103338, 2021.

787



788 Valavanidis, A., Fiotakis, K. and Vlachogianni, T.: Airborne particulate matter and human
789 health: Toxicological assessment and importance of size and composition of particles for
790 oxidative damage and carcinogenic mechanisms, *J. Environ. Sci. Heal. - Part C Environ.*
791 *Carcinog. Ecotoxicol. Rev.*, 26(4), 339–362, doi:10.1080/10590500802494538, 2008.
792
793 Wang, P., Xu, F., Gui, H., Wang, H. and Chen, D. R.: Effect of relative humidity on the
794 performance of five cost-effective PM sensors, *Aerosol Sci. Technol.*, 55(8), 957–974,
795 doi:10.1080/02786826.2021.1910136, 2021.
796
797 Weissert, L., Alberti, K., Miles, E., Miskell, G., Feenstra, B., Henshaw, G. S., Papapostolou, V.,
798 Patel, H., Polidori, A., Salmond, J. A. and Williams, D. E.: Low-cost sensor networks and land-
799 use regression: Interpolating nitrogen dioxide concentration at high temporal and spatial
800 resolution in Southern California, *Atmos. Environ.*, 223(January), 117287,
801 doi:10.1016/j.atmosenv.2020.117287, 2020.
802
803 Whitty, R. C. W., Pfeffer, M. A., Ilyinskaya, E., Roberts, T. J., Schmidt, A., Barsotti, S., Strauch,
804 W., Crilley, L. R., Pope, F. D., Bellanger, H., Mendoza, E., Mather, T. A., Liu, E., Peters,
805 N., Taylor, I. A., Francis, H., Hernandez Leiva, X., Lynch, D., Nobert, S., Baxter, P.:
806 Effectiveness of low-cost air quality monitors for identifying volcanic SO₂ and PM downwind
807 from Masaya volcano, Nicaragua. *Volcanica*, 2022 (In press).
808
809 WHO global air quality guidelines. Particulate matter (PM_{2.5} and PM₁₀), ozone, nitrogen
810 dioxide, sulfur dioxide and carbon monoxide, World Health Organisation, ISBN 978-92-4-
811 003443-3, Licence: CC BY-NC-SA 3.0 IGO, Geneva, 2021
812
813 Wu, S., Ni, Y., Li, H., Pan, L., Yang, D., Baccarelli, A. A., Deng, F., Chen, Y., Shima, M. and Guo,
814 X.: Short-term exposure to high ambient air pollution increases airway inflammation and
815 respiratory symptoms in chronic obstructive pulmonary disease patients in Beijing, China,
816 *Environ. Int.*, 94, 76–82, doi:10.1016/j.envint.2016.05.004, 2016.
817
818 Xu, Y., Zhang, J.S.: Understanding SVOCs, *ASHRAE Journal*, 53 (12), 121 - 125, 2011.
819



820 Zeger, S. L., Dominici, F., McDermott, A. and Samet, J. M.: Mortality in the medicare
821 population and Chronic exposure to fine Particulate air pollution in urban centers (2000-
822 2005), *Environ. Health Perspect.*, 116(12), 1614–1619, doi:10.1289/ehp.11449, 2008.
823



824 **FIGURE LEGENDS**

825

826 **Figure 1:** Map of the measuring station.

827

828 **Figure 2:** Particle profiles of the factors from the PMF analysis (> 500 nm). The lines
829 indicate the average particle count per second for each particle size bin.

830

831 **Figure 3:** Variable association for the factors from the LC analysis. Grey bars indicate
832 the values of F, while red bars indicate the explained variations for each
833 variable.

834

835 **Figure 4:** Temporal variation of the contributions of the factors from the LC analysis. The
836 windroses refer to the wind conditions for the corresponding periods when
837 specific factors presented higher G contributions.

838

839 **Figure 5:** Polar plot of the average G contributions of the factors from the LC analysis.

840

841 **Figure 6:** Average G contribution of the factors from the LC analysis for incoming air
842 masses. Higher contributions indicate better association of the given factor
843 with the corresponding air mass origin.

844

845 **Figure 7:** Variable association for the factors from the RG analysis. Grey bars indicate the
846 values of F, while red bars indicate the explained variations for each variable.

847

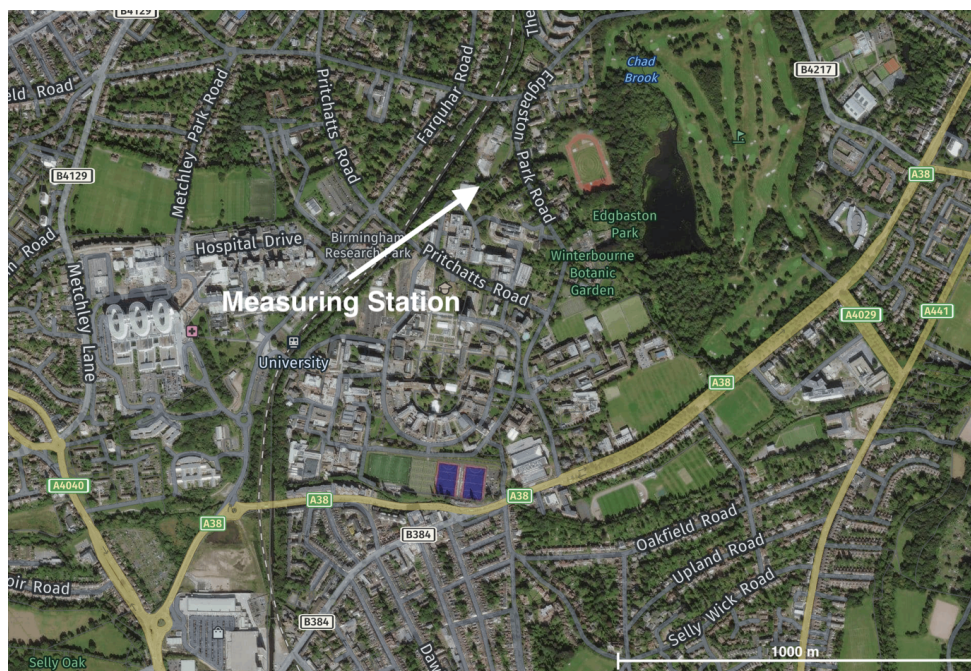
848 **Figure 8:** Polar plot of the average G contributions of the factors from the RG analysis.

849

850 **Figure 9:** Average G contribution of the factors from the RG analysis for incoming air
851 masses. Higher contributions indicate better association of the given factor
852 with the corresponding air mass origin.

853

854



855

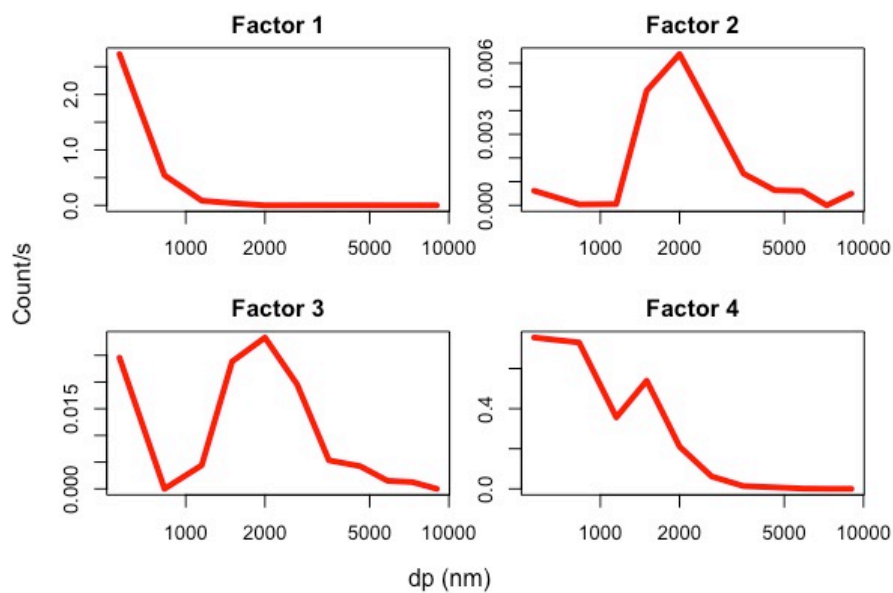
856 Figure 1: Map of the measuring station. Imagery ©2022 Bluesky, Getmapping plc, Infoterra
857 Ltd & Bluesky, Maxar Technologies, The GeoInformation Group, Map data
858 ©2022

859

860

861

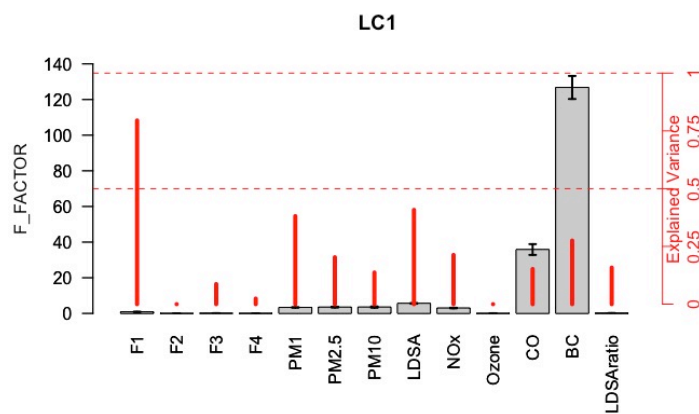
862



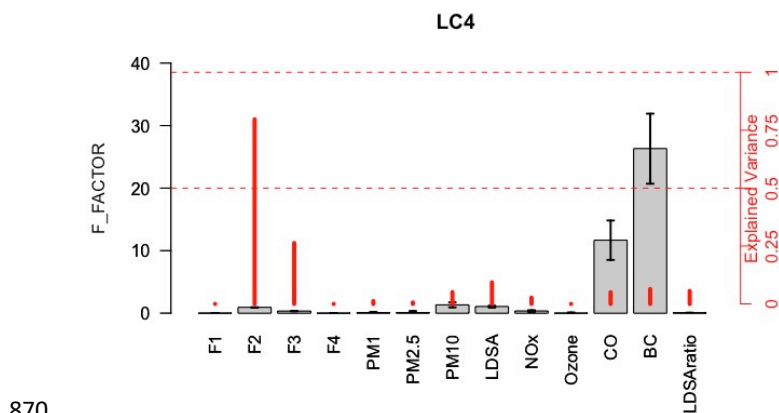
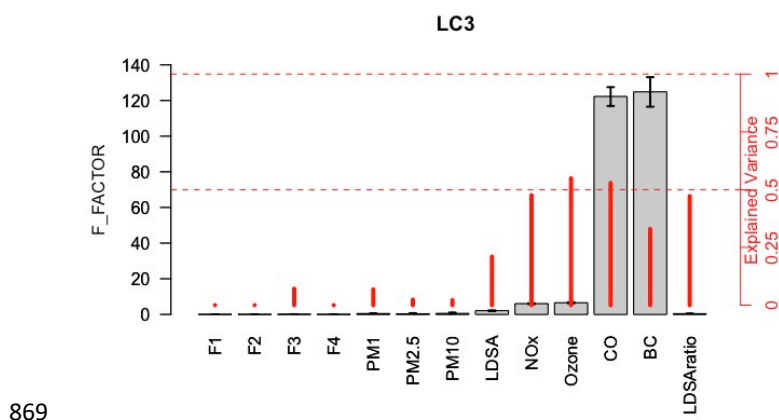
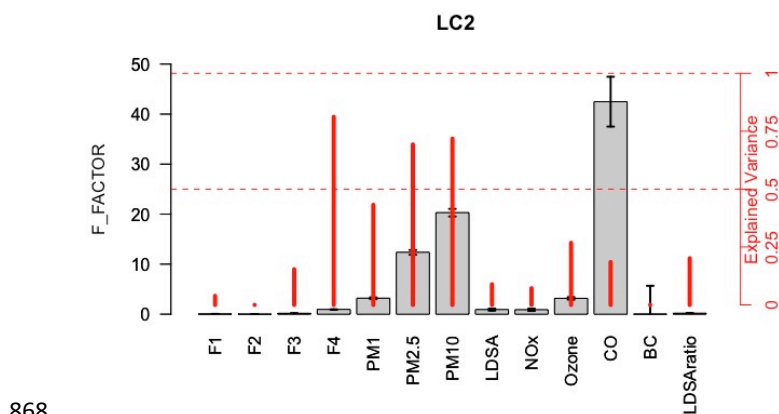
863

864 Figure 2: Particle profiles of the factors from the PMF analysis (above 500 nm). The lines
 865 indicate the average particle count per second for each particle size bin.

866

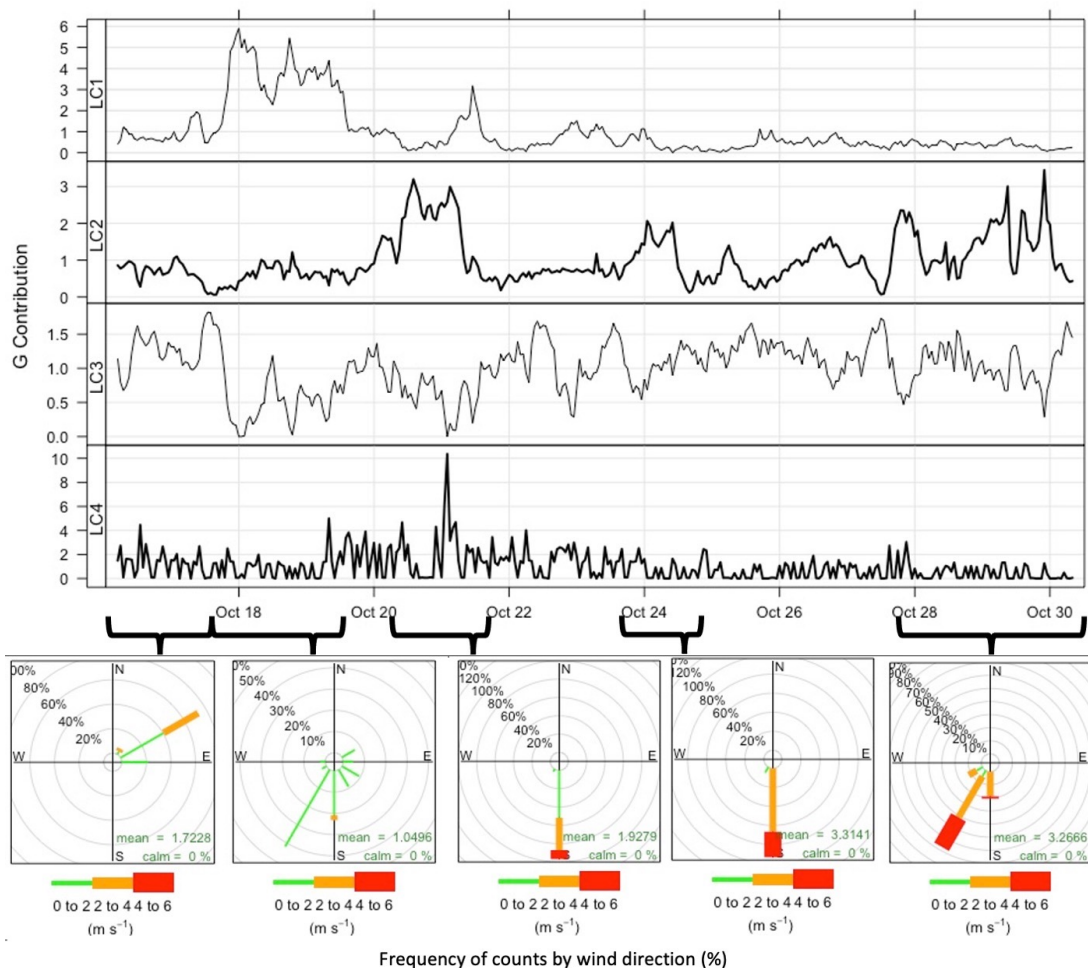


867



871 Figure 3: Contribution of the factors from the LC analysis. Grey bars indicate the values of F,
872 while red bars indicate the explained variations for each variable.

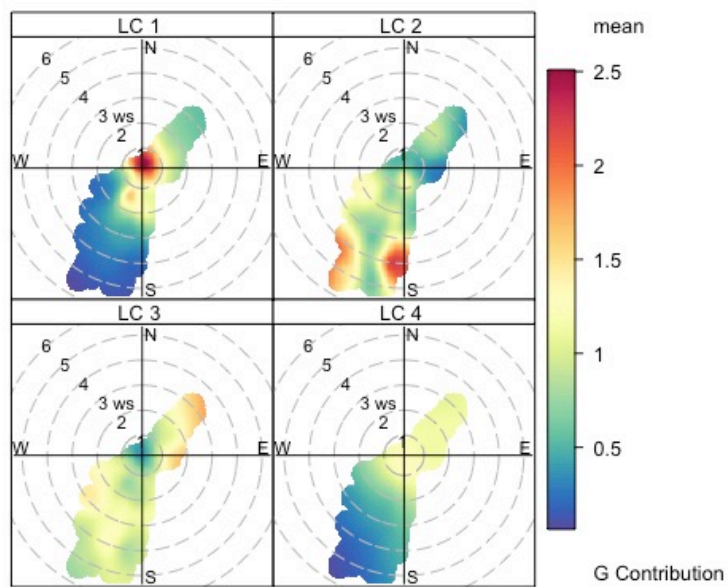
873



874

875 Figure 4: Temporal variation of the contributions of the factors from the LC analysis. The
876 windroses refer to the wind conditions for the corresponding periods when specific factors
877 presented higher G contributions.

878



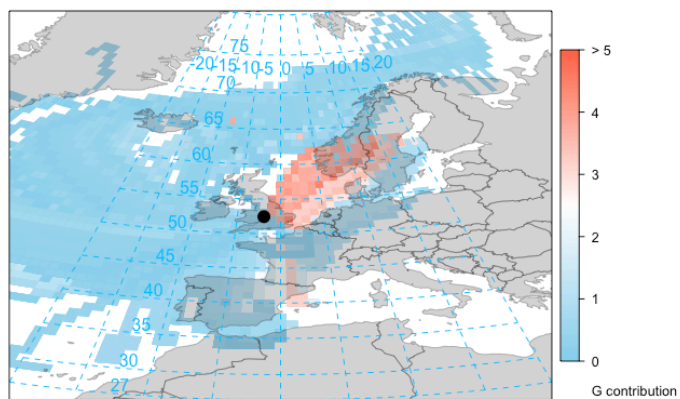
879

880 Figure 5: Polar plot of the average G contributions of the factors from the LC analysis.

881

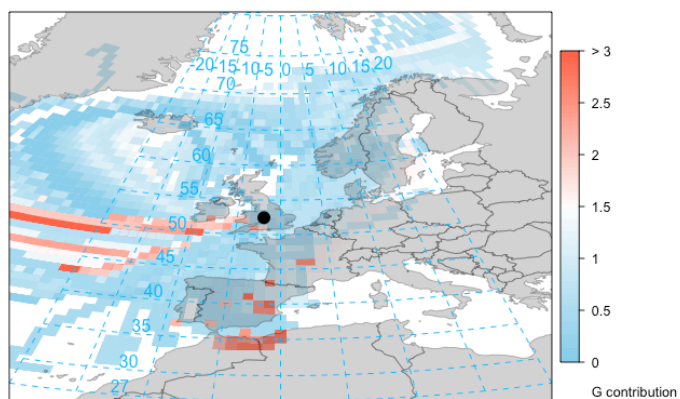


882



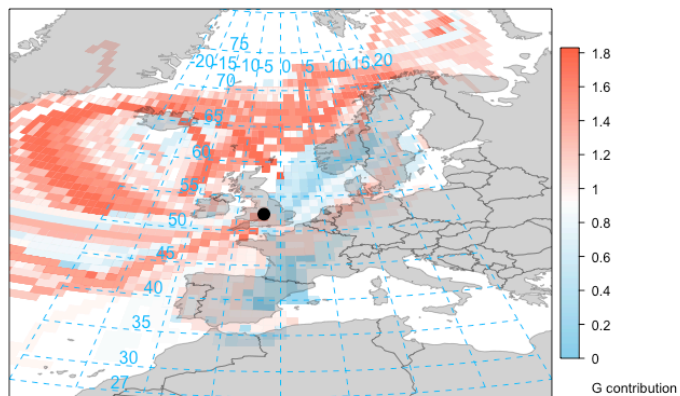
LC1

883

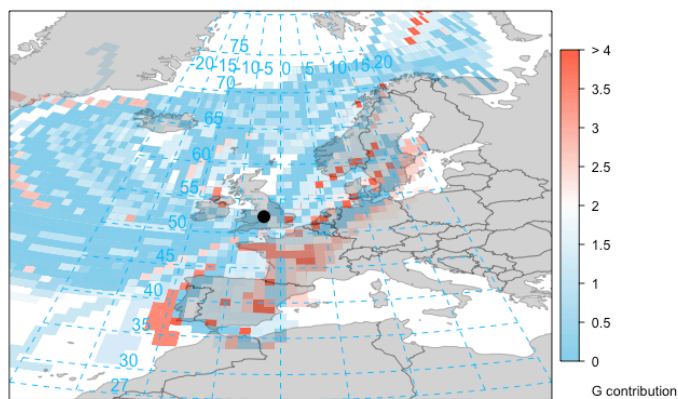


LC2

884



LC3



885

LC4

886 Figure 6: Average G contribution of the factors from the LC analysis for incoming air masses.

887 Higher contributions indicate better association of the given factor with the corresponding

888 air mass origin.

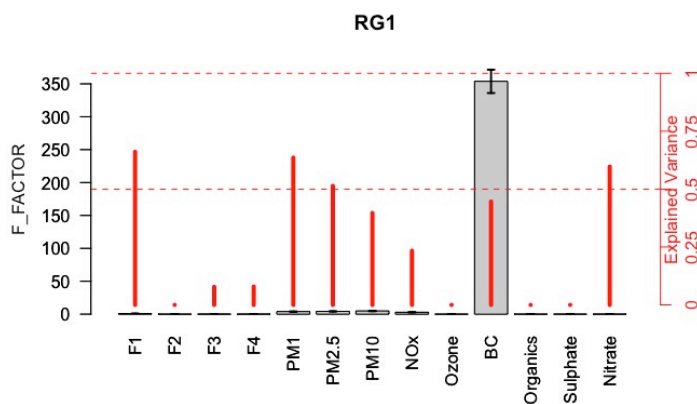
889

890

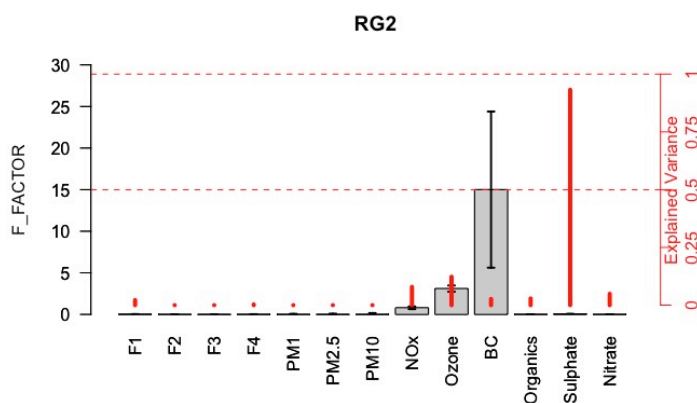
891



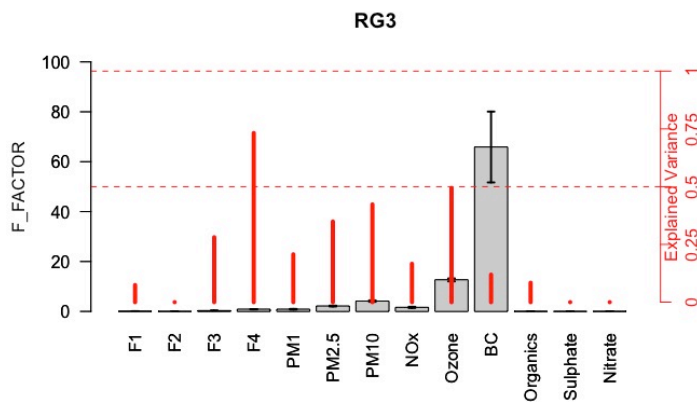
892
893

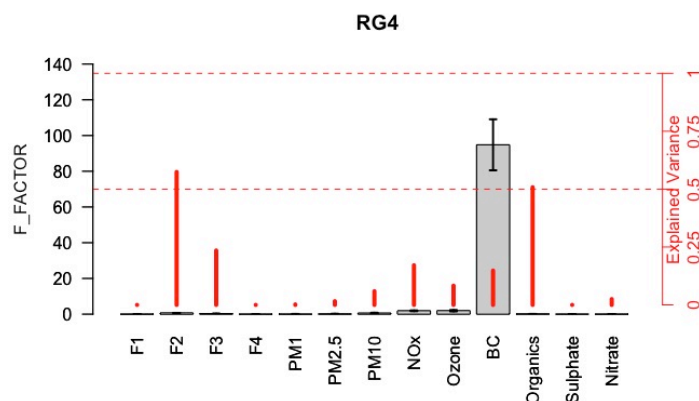


894



895



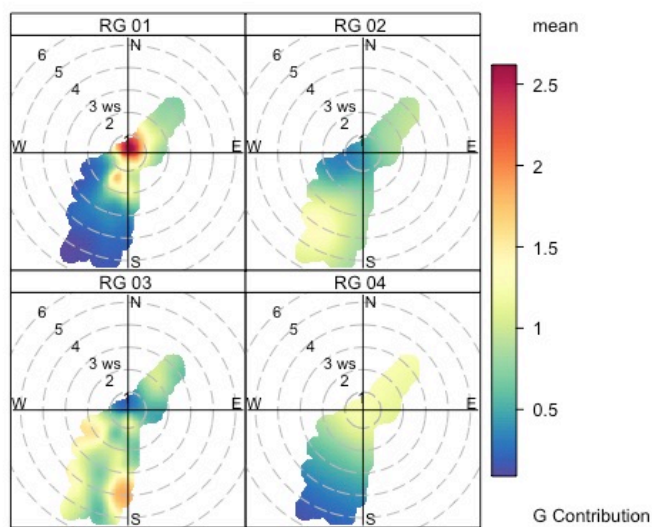


896

897 Figure 7: Variable association for the factors from the RG analysis. Grey bars indicate the
898 values of F, while red bars indicate the explained variations for each variable.

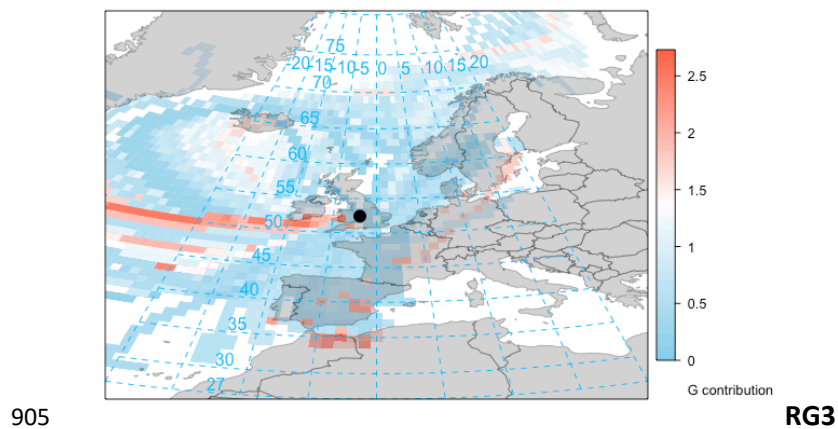
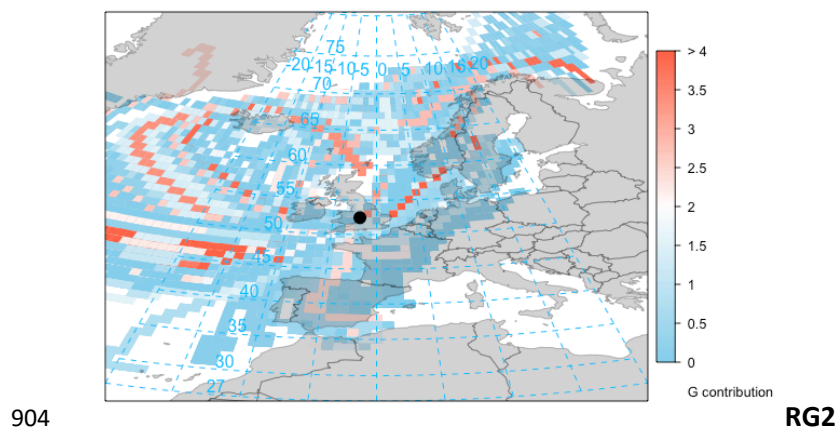
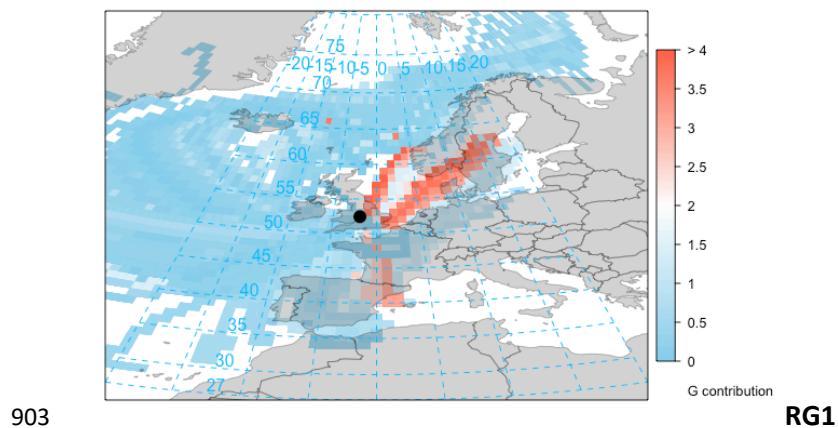
899

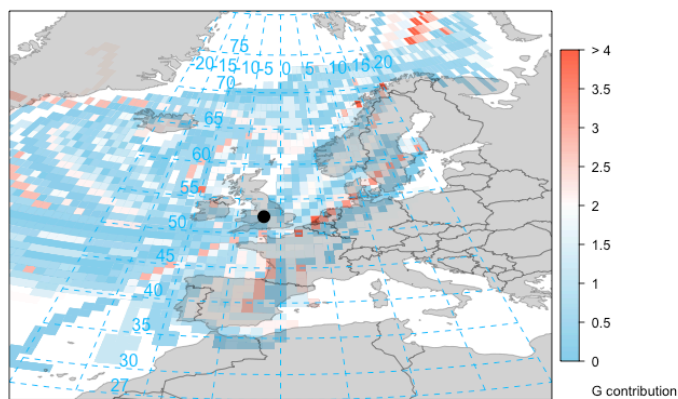
900



901

902 Figure 8: Polar plot of the average G contributions of the factors from the RG analysis.





906

RG4

907 Figure 9: Average G contribution of the factors from the RG analysis for incoming air masses.

908 Higher contributions indicate better association of the given factor with the corresponding

909 air mass origin.